Paper ID APEN-MIT-2019_125
Applied Energy Symposium: MIT A+B
May 22-24, 2019 • Boston, USA

Near-field radiative heat transfer enhanced by strongly-coupled surface polaritonic modes

W. B. Zhang
Institute of Engineering Thermophysics
Shanghai Jiao Tong University
Shanghai, China
wenbinzhang_2017@sjtu.edu.cn

B. X. Wang
Institute of Engineering Thermophysics
Shanghai Jiao Tong University
Shanghai, China
wangboxiang@sjtu.edu.cn

C. Y. Zhao*
Institute of Engineering Thermophysics
Shanghai Jiao Tong University
Shanghai, China
changying.zhao@sjtu.edu.cn

***Abstract*—** Surface polaritonic modes like surface plasmon polaritons (SPPs) and surface phonon polaritons (SPhPs) at interfaces can significantly enhance near-field radiative transfer between nanostructured surfaces. In this work, we study the near-field heat transfer between graphene/SiC composite nanostructures. It is demonstrated that thermally excited SPPs and SPhPs in such composite nanostructures lead to a significant enhancement in near-field heat transfer rate. To further analyze the underlying mechanisms, we calculate energy transmission coefficients and obtain the near-field dispersion relations. The dispersion relations of composite nanostructures are substantially different from those of isolated graphene or SiC films, which are due to the strong coupling effects between different polaritonic modes. We further identify four pairs of strongly coupled polaritonic modes with considerable Rabi frequencies, which mainly contribute to the enhancement in near-field heat transfer. This work provides a route to utilize strongly coupled surface polaritonic modes to manipulate near-field heat transfer, which has potential applications in waste heat recovery and heat management.

Keywords— near-field radiative transfer, strong coupling effect, frequency resonant mode, SPPs-SPhPs modes

I. Introduction

About 20-50% of the energy consumed in the industries enters the environment as waste heat in the form of hot exhaust gases, cooling water, and heat lost from hot equipment surfaces [1]. Harvesting this enormous amount of heat is thus of critical importance for improving the efficiency of energy usage and reducing carbon emissions. Thanks to the extremely high heat transfer enhancement, near-field radiative heat transfer (NFRHT) techniques including near-field thermophotovoltaics (NFTPV) [2] and near-field cooling [3] are promising in waste heat recovery [4], and thermal management applications [5].

Because of the tunneling effect of evanescent waves, NFRHT can exceed the blackbody radiation limit by several orders of magnitude [6], especially when surface plasmon polaritons (SPPs) or surface phonon polaritons (SPhPs) are excited [7]. Recently, graphene has been demonstrated to be a good candidate to support SPPs for low loss and excellent tunability from near-infrared to terahertz frequencies. It was shown that thermally excited SPPs can strongly mediate the NFRHT between graphene sheets [8]. When structures consist of graphene with other dielectric materials or metamaterials, the NFRHT can be further enhanced due to the coupling effects of different resonant modes [9-10]. However, it is still unclear how these coupling effects play a role in near-field heat transfer. In order to further understand and control the NFRHT in these systems, the mechanisms of excitation, coupling and interference of different frequency resonant modes (FSMs), which stand for branches of surface polaritonic modes, need to be comprehensively explored.

In this work, we study the NFRHT of three structures which are monolayer graphene, SiC film and graphene/SiC film composite structure in order to investigate the coupling effects on NFRHT. Surface polaritonic modes of these structures are excited in infrared region. To analyze the underlying mechanisms, we calculate energy transmission coefficients and obtain the near-field dispersion relations. Due to the strong coupling effects between different polaritonic modes, the dispersion relations of composite structures are substantially different from those of isolated graphene or SiC films. Additionally, we further identify four pairs of strongly coupled polaritonic modes with considerable Rabi frequencies. This work provides a route to enhance near-field heat transfer by strongly coupled surface polaritonic modes, promising in waste heat recovery and heat management.

II. Theory

The schematic of NFRHT between graphene/SiC film composite structures is illustrated in Fig. 1. Based on fluctuational electrodynamics using dyadic Green's functions, the heat flux between two structures can be calculated by [11]:

$$Q = \frac{1}{4\pi^2}\int_0^\infty \left[\Theta(T_E,\omega)-\Theta(T_R,\omega)\right]d\omega \int_0^\infty \beta \sum_{j=s,p} \xi_j(\omega,\beta)\,d\beta, \quad (1)$$

where the local thermal equilibrium temperatures T_E and T_R are identified as the emitter and the receiver, respectively. β is the lateral wave vector of thermal radiation waves and d indicates the vacuum gap distance, $j = s, p$ stands for *s*- or *p*-polariton modes, respectively. $\Theta(T,\omega) = \hbar\omega / \left[\exp\left(\hbar\omega / k_B T\right) - 1\right]$ is the mean energy of thermal harmonic oscillators.

Fig. 1. Schematic of NFRHT between graphene/SiC composite structures. The parameter *d* means the vacuum gap distance of NFRHT and the thickness of SiC film can be controlled by the *h*.

The energy transmission coefficient $\xi_j(\omega,\beta)$ is given by [12-13]:

$$\xi_j(\omega,\beta)=\begin{cases}\dfrac{\left(1-\left|r_{j,E}\right|^2\right)\left(1-\left|r_{j,R}\right|^2\right)}{\left|1-r_{j,E}r_{j,R}e^{2ik_{z0}d}\right|^2}, & \beta<k_0\\ \dfrac{4\,\mathrm{Im}\left(r_{j,E}\right)\mathrm{Im}\left(r_{j,R}\right)e^{-2|k_{z0}|d}}{\left|1-r_{j,E}r_{j,R}e^{2ik_{z0}d}\right|^2}, & \beta>k_0\end{cases} \quad (2)$$

where $r_{j,E}$ and $r_{j,R}$ indicate Fresnel reflection coefficients of the emitter and receiver, respectively. $k_{z0}=\left(k_0^2-\beta^2\right)^{1/2}$ denotes the *z*-component of the wave vector in vacuum. Note in Eq. (2), the expressions of energy transmission coefficients for propagating waves ($\beta<k_0$) and evanescent waves ($\beta>k_0$) are different.

The Fresnel reflection coefficients for the graphene covered composite structures are calculated by the following forms:

$$r_{p,l}=\frac{r_{12,p}+\left(1-r_{12,p}-r_{21,p}\right)r_{21,p}e^{2ik_{z,2}h}}{1-r_{21,p}r_{23,p}e^{2ik_{z,2}h}},\quad r_{s,l}=\frac{r_{12,s}+\left(1+r_{12,s}+r_{21,s}\right)r_{21,s}e^{2ik_{z,2}h}}{1-r_{21,s}r_{23,s}e^{2ik_{z,2}h}} \quad (3)$$

where 1, 2, and 3 are the indexes for the vacuum region above SiC film, in the SiC film, and the vacuum region below SiC film, respectively, as shown in Fig. 1. Besides, the *l* = *E* or *R* stands for the emitter or receiver and *h* means the thickness of SiC film. As for Eq. (3), it can also be used for structures with only monolayer graphene by setting r_{23} = 0.

For a dielectric material which is covered by a monolayer graphene, the Fresnel reflection coefficients become:

$$r_{ab,s,l}=\frac{k_{z,a}-k_{z,b}-\sigma\mu_0^2\omega}{k_{z,a}+k_{z,b}+\sigma\mu_0^2\omega},\quad r_{ab,p,l}=\frac{k_{z,a}\varepsilon_{\perp,b}-k_{z,b}\varepsilon_{\perp,a}+\sigma k_{z,a}k_{z,b}/\varepsilon_0\omega}{k_{z,a}\varepsilon_{\perp,b}+k_{z,b}\varepsilon_{\perp,a}+\sigma k_{z,a}k_{z,b}/\varepsilon_0\omega} \quad (4)$$

where $k_{z,n}=\left(\varepsilon_{\perp,n}k_0^2-\varepsilon_{\perp,n}\beta^2/\varepsilon_{\parallel,n}\right)^{1/2}$ with *n* = 1, 2, or 3 in Eq. (3) and Eq. (4). $\varepsilon_\perp$ and $\varepsilon_\parallel$ are the vertical and parallel components of the relative dielectric tensor. If there is a monolayer graphene between media *a* and *b*, where *a* = 1, 2 and *b* = 1, 2 or 3. The role of a monolayer graphene can be regarded as a current sheet. σ is the conductivity of graphene. If there is only SiC film, σ in Eq. (4) should be set to be zero. Since in the mid- and far-infrared region, σ is dominated by the intraband transitions, where it can be calculated as [14]:

$$\sigma=\frac{e^2\mu}{\pi\hbar^2}\frac{\tau}{1-i\omega\tau}. \quad (5)$$

SiC film is a nonmagnetic polar material. According to Lorentz model, the dielectric function of SiC is given by [15]:

$$\varepsilon_{SiC}=\varepsilon_\infty\frac{\omega^2-\omega_{LO}^2+i\Gamma\omega}{\omega^2-\omega_{TO}^2+i\Gamma\omega}. \quad (6)$$

ω_{LO} and ω_{TO} are longitudinal optical phonon frequency and transverse optical phonon frequency, respectively. The parameters in Eq. (6) can refer to the materials handbook [15].

III. Results and Discussion

A. Large enhancement of NFRHT between composite structures

In this work, thermal equilibrium temperatures of the emitter and receiver are T_E = 310 K and T_R = 290 K, respectively. According to Eq. (1), we can obtain the heat flux of different structures (illustrated in Fig. 2). Based on NFRHT of the three structures, the graphene/SiC film composite structures have the highest total heat flux which is 344.5 kW/m^2 when the gap distance is 20 nm. Due to the exponentially decaying feature of large-wave-vector evanescent waves, the heat flux of graphene/SiC film composite structures decreases faster than monolayer graphene structure. When the gap distance is about 5000 nm, the heat fluxes of three structures are almost the same, approaching the far-field region. Besides, when the vacuum gap distance between two graphene/SiC film composite structures is less than 100 nm, the total heat flux can exceed the Planck's thermal radiation above 500 times, which can therefore greatly enhance the efficiency of waste heat recovery and heat management.

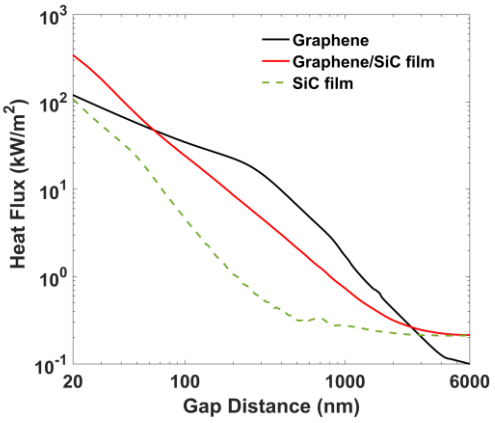

Fig. 2. Heat flux versus vacuum gap distance *d* from 20 to 6000 nm of different structures. Chemical potential of graphene is μ = 0.3 eV. Thickness of SiC film is *h* = 50 nm.

B. Near-field energy transmission coefficient

Mechanisms for the enhancement of NFRHT between composite structures can be analyzed by the contours of energy transmission coefficient, which are shown in Fig. 3. The transverse wave vector is normalized by $\beta_0=\omega_0/c$ with $\omega_0=1\times10^{14}\,rad/s$. The bright bands presented in Fig. 3 demonstrate higher photon tunneling rate arising from the excitation of different surface polaritonic modes. According to Fig. 3a, there are two bright bands separated in the low-frequency region and converging in the high-frequency region, which are coupled SPPs between the two monolayer graphene structures. Fig. 3b presents bright bands which are thermally excited SPhPs near the frequency of SiC-vacuum interface [16]. In the enlarged dispersion relations shown in the inset of Fig. 3b, it is observed that there are four FRMs, which converge in the high-transverse-wave-vector region.

The energy transmission coefficient of graphene/SiC film composite structure is presented in Fig. 3c. It is seen that bright bands split into two branches because SPhPs excited in isotropic polar materials (SiC film) couple with SPPs in graphene, resulting in SPPs-SPhPs hybrid modes. Similar phenomena were observed in the coupling between SPPs in graphene or thin metal layer with the SPhPs in SiO_2 substrates [17]. However, the SPhPs modes excited near the frequency of 1.786×10^{14} rad/s (frequency of SiC vacuum interface) are attenuated appreciably compared with those in Fig. 3b. In the high-transverse-wave-vector region, SPhPs almost disappear. This phenomenon is also a manifestation of the strong coupling effect NFRHT between graphene/SiC film composite structures, which can induce a photonic gap without any modes.

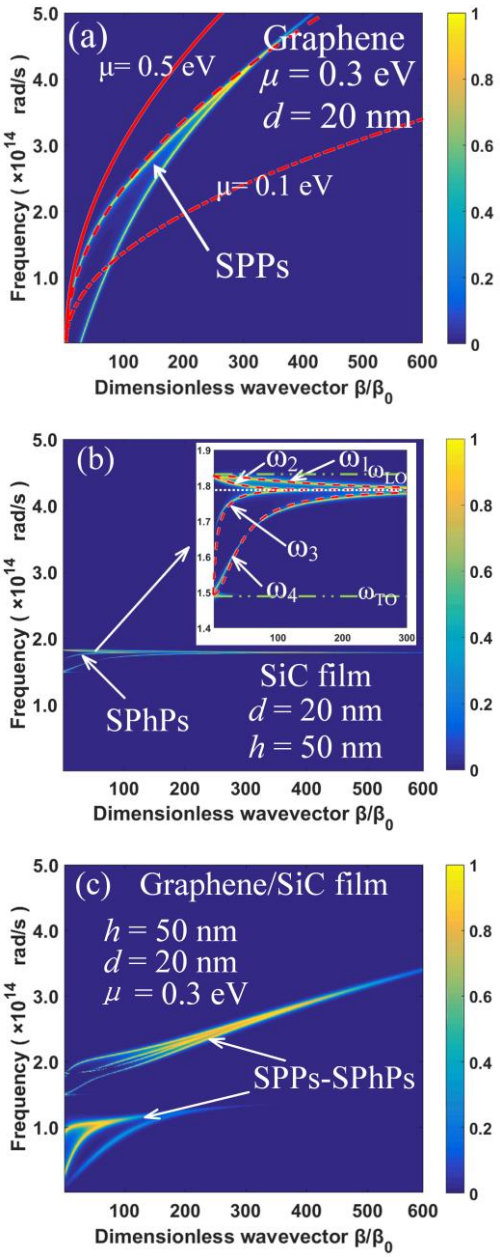

Fig. 3. Energy transmission coefficient contours for different structures.

C. Asymptotic analysis of FRMs

To further examine the origin and consequences of the strong coupling effect, here we first carry out an asymptotic analysis of the near-field dispersion relations. Through the Eq. (2), the radiative heat flux diverges when the following condition is fulfilled:

$$1-r_{j,E}r_{j,R}e^{2ik_{z0}d}=0. \tag{7}$$

We can obtain each FSM by solving the Eq. (7).

In terms of dielectric materials like SiC film with isotropic optical properties, for surface wave with $\beta\gg k_0$, the z-component of the wave vector is $k_{z,n}=\left(\varepsilon_{\perp,n}k_0^2-\varepsilon_{\perp,n}\beta^2/\varepsilon_{\parallel,n}\right)^{1/2}$ with n = 1, 2, or 3, which can be approximated as $k_{z,n}\approx i\beta$. Ignoring the imaginary part of Eq. (7), we can get $r_{12}=S(\beta,h,d)$, where S is satisfied with the following condition:

$$S(\beta,h,d)=\pm\sqrt{\frac{-b\pm\sqrt{b^2-4ac}}{2a}}, \tag{8}$$

$$\begin{cases} a=e^{\beta(d-2h)} \\ b=2e^{-\beta d}-2e^{\beta d}-e^{-\beta(d+2h)}-e^{-\beta(d-2h)} \\ c=e^{\beta(d+2h)} \end{cases}. \tag{9}$$

By using dielectric function of SiC film in Eq.(6), the FRMs of SiC film can be obtained as

$$\omega_S\approx\left[\frac{S\left(\varepsilon_\infty\omega_{LO}^2+\omega_{TO}^2\right)+\left(\omega_{TO}^2-\varepsilon_\infty\omega_{LO}^2\right)}{S\left(\varepsilon_\infty+1\right)+\left(1-\varepsilon_\infty\right)}\right]^{1/2}, \tag{10}$$

where the losses are small and thus ignored. Eq. (10) offers an approximation of the four FRMs of the two film structures as a function of d, h, and β. From Eq. (10), the resonant frequencies where the radiative heat flux between two SiC film structures has the maximal value can be determined, shown as red dashed lines in Fig. 3b. The analytical formulas can accurately predict each FRM. ω_1 corresponds to the highest FRM and ω_4 is consistent with the lowest FRM. The horizontal white dotted line means the frequency of SiC-vacuum interface. The horizontal green dot-dash lines are longitudinal optical phonon frequency and transverse optical phonon frequency, respectively. These three lines are the limits of the SPhPs near-field dispersion relation of SiC film structures.

Fig.3a (red lines) depicts the near-field dispersion relation of SPPs for a monolayer graphene for three selected values of the chemical potential. These parabolic curves can be described by the Eq. (11) [18]:

$$\beta(\omega)=\frac{2\hbar\omega^2\eta}{g\alpha\mu V_F}, \tag{11}$$

where the parameters in Eq. (11) can refer to Ref.[18]. Obviously, with the increase of the chemical potential of graphene, the SPPs cannot occur at the high-transverse-wave-vector region, which is disadvantageous to the NFRHT enhancement.

D. Strong coupling of SPPs-SPhPs modes in graphene/SiC film composite structures

Based on the analytical formulas in Section III.C, here in this subsection, we further investigate the effects of coupling modes on NFRHT enhancement. All the parameters used here are the same as those in Fig. 3. As illustrated in Fig. 4a, both monolayer graphene and SiC film show only one narrow peak corresponding to the thermally excited SPPs and SPhPs. The spectral heat flux of

graphene/SiC film composite structure (red solid line) has two peaks, which are generated from the strong coupling of SPPs-SPhPs modes that generate hybrid modes. The low frequency peak is at 1.07×10^{14} rad/s and the high frequency peak is at 2.23×10^{14} rad/s. These two peak frequencies are substantially different with the optical phonon frequencies of the SiC film, which suggests that strong coupling indeed takes place in graphene/SiC film composite structures. Moreover, the strong coupling effect can greatly broaden the spectral peak.

Fig. 5b explicitly shows the strong coupling between the SPPs and SPhPs modes, in which two dispersive branches featuring anti-crossing (splitting) are shown as two bright bands. Four red lines mean the FRMs of SPhPs given by the Eq. (10). The parabolic green dot-dash line means graphene SPPs mode given by the Eq. (11). By solving the cross points of SPPs mode and SPhPs mode, we can get four strong coupling Rabi frequencies which are $\Omega_1 = 9.9\times10^{13}$ rad/s, $\Omega_2 = 8.7\times10^{13}$ rad/s, $\Omega_3 = 8.3\times10^{13}$ rad/s, $\Omega_4 = 1.12\times10^{14}$ rad/s, which denote the emergent four pair strongly coupled modes. Therefore, it is those strongly coupled polaritonic modes that significantly enhance near-field radiative heat transfer.

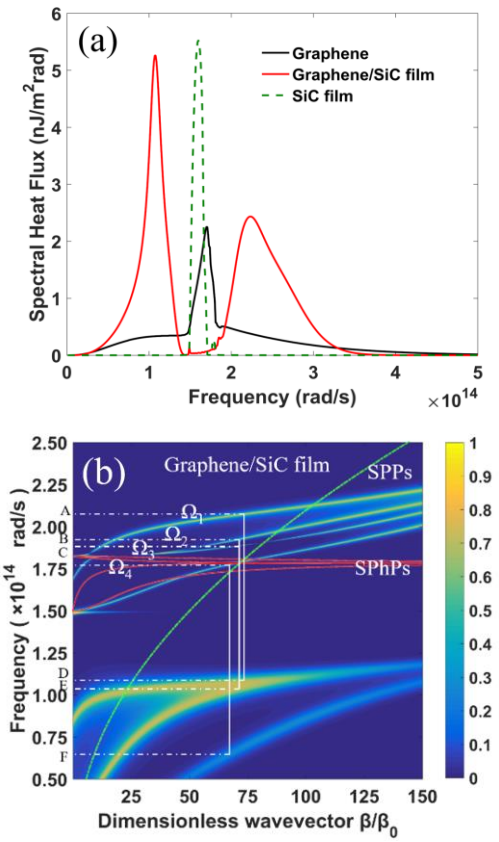

Fig. 4. (a) Spectral heat flux from different structures. (b) The energy transmission coefficient contours for graphene/SiC film composite structures.

IV. Conclusion

In this work, we study the near-field heat transfer between graphene/SiC composite nanostructures. It is demonstrated that thermally excited SPPs and SPhPs in such composite nanostructures lead to a significant enhancement in near-field heat transfer rate. To further analyze the underlying mechanisms, we calculate energy transmission coefficients and obtain the near-field dispersion relations. The dispersion relations of composite nanostructures are substantially different from those of isolated graphene or SiC films, which are due to the strong coupling effects between different polaritonic modes. We further identify four pairs of strongly coupled polaritonic modes with considerable Rabi frequencies, which mainly contribute to the enhancement in near-field heat transfer. This work provides a route to utilize strongly coupled surface polaritonic modes to manipulate near-field heat transfer, which has potential applications in waste heat recovery and heat management.

.

Acknowledgment

This work is supported by the National Natural Science Foundation of China (Grant No.51636004), Shanghai Key Fundamental Research Grant (No.18JC1413300, No.16JC1403200) and the Foundation for Innovative Research Groups of the National Science Foundation of China (Grant No. 51521004).

References

[1] BCS I. Waste heat recovery: technology and opportunities in US Industry[J]. Industrial technologies program, US Department of Energy, 2008.

[2] Fiorino A, Zhu L, Thompson D, et al. Nanogap near-field thermophotovoltaics[J]. Nature nanotechnology, 2018, 13(9): 806.

[3] Lin C, Wang B, Teo K H, et al. A coherent description of thermal radiative devices and its application on the near-field negative electroluminescent cooling[J]. Energy, 2018, 147: 177-186.

[4] Zhao B, Santhanam P, Chen K, et al. Near-Field Thermophotonic Systems for Low-Grade Waste-Heat Recovery[J]. Nano letters, 2018, 18(8): 5224-5230.

[5] Lim M, Song J, Lee S S, et al. Tailoring near-field thermal radiation between metallo-dielectric multilayers using coupled surface plasmon polaritons[J]. Nature communications, 2018, 9(1): 4302.

[6] Kralik T, Hanzelka P, Zobac M, et al. Strong near-field enhancement of radiative heat transfer between metallic surfaces[J]. Physical Review Letters, 2012, 109(22):224302.

[7] Liu X, Zhang R Z, Zhang Z. Near-Perfect Photon Tunneling by Hybridizing Graphene Plasmons and Hyperbolic Modes[J]. Acs Photonics, 2014, 1(9):785-789.

[8] Ilic O , Jablan M , Joannopoulos J , et al. Near-field thermal radiation transfer controlled by plasmons in graphene[J]. Physical Review B, 2012, 85(15):155422-0.

[9] Messina R, Ben-Abdallah P, Guizal B, et al. Graphene-based amplification and tuning of near-field radiative heat transfer between dissimilar polar materials[J]. Physical Review B, 2017, 96(4): 045402.

[10] Zhao Q, Zhou T, Wang T, et al. Active control of near-field radiative heat transfer between graphene-covered metamaterials[J]. Journal of Physics D: Applied Physics, 2017, 50(14): 145101.

[11] Liu X L, Bright T J, Zhang Z M. Application Conditions of Effective Medium Theory in Near-Field Radiative Heat Transfer Between Multilayered Metamaterials[J]. Journal of Heat Transfer, 2014, 136(9):092703.

[12] Ito K, Nishikawa K, Miura A, et al. Dynamic Modulation of Radiative Heat Transfer beyond the Blackbody Limit[J]. Nano Letters, 2017, 17(7):4347.

[13] Ikeda T, Ito K, Iizuka H. Tunable quasi-monochromatic near-field radiative heat transfer in s and p polarizations by a hyperbolic metamaterial layer[J]. Journal of Applied Physics, 2017, 121(1):013106.

[14] Zhao B, Zhang Z M. Strong Plasmonic Coupling between Graphene Ribbon Array and Metal Gratings[J]. Acs Photonics, 2015, 2(11).

[15] Palik E D. Handbook of optical constants of solids II[J]. Boston Academic Press, 1991, 1(1):77-135.

[16] Francoeur M , M. Pınar Mengüç, Vaillon R . Spectral Tuning of Near-field Radiative Heat Flux between Two Thin Silicon Carbide Films[J]. Journal of Physics D Applied Physics, 2010, 43(7).

[17] Messina R, Hugonin J P, Greffet J J, et al. Tuning the electromagnetic local density of states in graphene-covered systems via strong coupling with graphene plasmons[J]. Physical Review B Condensed Matter, 2013, 87(87):173-177.

[18] B Wunsch, T Stauber, F Sols, et al. Dynamical polarization of graphene at finite doping[J]. New Journal of Physics, 2006, 8:318.